Ferroelectric phase transition, ionicity condensation, and multicriticality in charge-transfer organic complexes

Ferroelectric phase transition, ionicity condensation, and multicriticality in charge-transfer organic complexes

Jun-ichiro Kishine,[1] Tadeusz Luty,[2] and Kenji Yonemitsu,[1]
[1]*Department of Theoretical Studies, Institute for Molecular Science, Okazaki 444-8585, Japan and Department of Functional Molecular Science, Graduate University for Advanced Studies, Okazaki 444-8585, Japan*
[2]*Institute of Physical and Theoretical Chemistry, Technical University of Wrocław, 50-370 Wrocław, Poland*
(Received 12 July 2003; revised manuscript received 3 November 2003; published 27 February 2004)

To elucidate a pressure-temperature phase diagram of the quasi-one-dimensional mixed-stack charge-transfer complex tetrathiafulvalene-*P*-chloranil (TTF-CA), we study the quasi-one-dimensional spin-1 Blume-Emery-Griffiths model. In addition to the local charge-transfer energy (Δ) and the inter-stack polar (dipole-dipole) interaction ($J_\perp$), we take account of the interstack electrostriction (Coulomb-lattice coupling). Using the self-consistent chain-mean-field theory, where the intra-stack degrees of freedom are exactly treated by the transfer-matrix method, we reproduce the gas-liquid-solid like phase diagram corresponding to the neutral (N), paraelectric ionic ($I_{\rm para}$), and ferroelectric ionic ($I_{\rm ferro}$) phases, respectively. Our classical model describes an essential point of the multicritical behavior of TTF-CA, i.e., the interchain electrostriction exclusively enhances the charge concentration (ionicity condensation), but does not affect the interchain ferroelectric coupling. This effect leads to appearance of the intermediate $I_{\rm para}$ phase in between the N and $I_{\rm ferro}$ phases on the Δ-T phase diagram.

DOI: 10.1103/PhysRevB.69.075115 PACS number(s): 77.84.Jd, 81.30.Dz, 61.50.Ks, 77.22.−d

I. INTRODUCTION

In the ''critical phase control technology,'' condensed molecular materials play quite a promising role, because molecular orbitals and stacking architecture are manipulable in a desirable way. To elucidate interrelation of constituent molecular structures and emergence of various@thermodynamic phases such as superconductivity, magnetism, and ferroelectricity is of great interest there. A neutral-to-ionic phase transition (NIT) in quasi-one-dimensional charge-transfer (CT) complexes comprising mixed-stack architecture of electron donor (D) and accepter (A) molecules[1] has played a key role in this field.

In particular, phase control by pressure[2,3] or laser radiation[4,3] in the tetrathiafulvalene-*p*-chloranil (TTF-CA), which exhibits the NIT around 80 K at ambient pressure, has attracted a great deal of interest. Very recently, Collet *et al.*,[5] using highly refined time-resolved x-ray diffraction technique, have reported direct observation of a photoinduced paraelectric-to-ferroelectric structural order in the crystal. In the ionic phase, the D^+A^- pair forms a dimer due to the electrostatic instability[6] or subsequent spin-Peierls instability.[7] The ionized dimer on the DA chain carries a local electric dipole moment p with opposite directions depending on the dimerization patterns $\underline{D^+A^-}$ or $\underline{A^-D^+}$. Once p acquires a macroscopic mean value $\eta=\langle p\rangle\neq 0$, a spontaneous inversion symmetry breaking (SISB) occurs and the system undergoes a phase transition to a ferroelectric-ionic ($I_{\rm ferro}$) phase. The ionic phase itself is simply described by ionicity condensation $c=\langle p^2\rangle\sim 1$. *Since η is a symmetry-breaking order parameter but c* is not, we expect that η and c play separate roles. The appearance of two distinct order parameters η and c is a direct consequence of the degeneracy of the two configurations of dimerization pattern, IA ($\cdots\underline{D^+A^-}\,\underline{D^+A^-}\cdots$) and IB ($\cdots\underline{A^-D^+}\,\underline{A^-D^+}\cdots$).

Recently, the respective roles of c and η have been highlighted in both equilibrium[2] and nonequilibrium[3] processes. Using the neutron diffraction along with nuclear-quadrupole-resonance measurements, Lemée-Cailleau *et al.*[2] found a phase where *the system is ionic but dipoles remain disordered*, i.e., a paraelectric ionic ($I_{\rm para}$) phase. They proposed a pressure-temperature phase diagram of TTF-CA, where the N, $I_{\rm para}$, and $I_{\rm ferro}$ phases are like gas, liquid, and solid phases, respectively. The ferroelectric order is well signaled by the appearance of $(0,2k+1,0)$ Bragg peaks that indicate the inversion symmetry breaking. The ''sublimation'' line separating the N and $I_{\rm ferro}$ phases continues up to a triple point $(P_t,T_t)\sim$(500 MPa, 210 K). Above the triple point, in addition to the ''crystallization (or melting)'' line, there appears a ''condensation'' line separating the $I_{\rm para}$ and N phases accompanied by a concomitant discontinuous change of c, ending at a critical point $(P_c,T_c)\sim$(700 MPa, 250 K). The purpose of this paper is to give a qualitative understanding of this phase diagram, as we later calculate in Fig. 5.

Since the SISB is prohibited by thermal fluctuations in a purely one-dimensional stack, interstack coupling is required to realize the SISB. In addition, the experimental observation strongly indicates that electronic and lattice degrees of freedom are coupled with each other in a unique manner. That is to say, upon crossing the transition lines in the gas-liquid-solid like phase diagram,[2,3] the unit cell parameter b (for the axis perpendicular to the stack) exhibits about 0.5% discontinuous contraction at the condensation transition but exhibits continuous contraction at the crystallization transition. On the other hand, the unit cell parameter a (for the stacking axis) exhibits only continuous contraction at the condensation transition and below it remains almost constant.[3] Now we are ready to ask the question: (1) what kind of interstack interactions are responsible for the occurrence of the $I_{\rm ferro}$ phase, and (2) how the lattice anomalies are coupled to the phase transitions ?

As for the first question, Luty *et al.*[3,8] stressed that the interstack non-polar coupling[7] alone cannot drive the ferroelectric ordering and the *dipolar* coupling plays an essential role. As for the second question, Kawamoto *et al.*[9] took account of the charge distribution on the atoms inside each molecule by an *ab initio* quantum chemical method and elucidated the importance of interstack Coulomb attraction ~ -0.14 eV, which may cause interstack electrostriction (Coulomb-lattice coupling).

II. QUASI-ONE-DIMENSIONAL BLUME-EMERY-GRIFFITHS MODEL AND INTERCHAIN MEAN-FIELD THEORY

Now we shall set up a model. The ground-state energy of the mixed stacks has three minima as a function of the dimerization displacement, i.e., the *N* and the degenerate IA and IB states. The three states may be described by the spin-1 Ising variable $p_{i,j}=0,\pm 1$ on the ith dimer inside the jth stack.[2,3,8] The charge transfer energy (Δ), the intrastack (with subscript $\|$) and interstack (with subscript $\perp$) dipolar (J) and nonpolar (K) interactions, and the coupling with the electric field (E) are described by the quasi-one-dimensional (Q1D) Blume-Emery-Griffiths (BEG) model,[10] $\mathcal{H}=\mathcal{H}_{\|}+\mathcal{H}_{\perp}$, where

$$\mathcal{H}_{\|}=-\sum_{i,j}\left[J_{\|}p_{i,j}p_{i+1,j}+K_{\|}p_{i,j}^2p_{i+1,j}^2-\Delta p_{i,j}^2-Ep_{i,j}\right], \tag{1}$$

$$\mathcal{H}_{\perp}=-\sum_{i,j}\left[J_{\perp}p_{i,j}p_{i,j+1}+K_{\perp}p_{i,j}^2p_{i,j+1}^2\right]. \tag{2}$$

The intrastack dipolar interaction $J_{\|}$ is caused by coupling between the charge transfer and the lattice distortion,[8] while the interstack dipolar interaction is regarded as a direct interaction between the induced dipoles on adjacent stacks. The intrastack couplings are much stronger than the interstack couplings, and the electric dipoles are aligned along the stacks. The energy cost to create one D^+A^- pair is given in the limit of no molecular overlap by $\Delta=I-A-\alpha V$, where I and A denote the donor's ionization energy and the acceptor's affinity, respectively, and αV denotes the Madelung energy.[11] Generally speaking, increasing pressure decreases the lattice spacing a and consequently increases V. Therefore, Δ decreases upon applying pressure.

We treat the Hamiltonian (2) by using the self-consistent chain-mean-field theory.[12] Introducing the thermal averages, $\eta=\langle p_{i,j}\rangle$ and $c=\langle p_{i,j}^2\rangle$, we have the effective 1D BEG model,

$$\mathcal{H}_{\|}^{\mathrm{eff}}=-\sum_{i}\left[J_{\|}p_ip_{i+1}+K_{\|}p_i^2p_{i+1}^2-\tilde{\Delta}p_i^2-\tilde{E}p_i\right]+\frac{z_{\perp}}{2}NJ_{\perp}\eta^2+\frac{z_{\perp}}{2}NK_{\perp}c^2, \tag{3}$$

where $\tilde{\Delta}=\Delta-z_{\perp}K_{\perp}c$ and $\tilde{E}=E-z_{\perp}J_{\perp}\eta$, with $z_{\perp}=2$ being the interstack coordination number. Treating $\mathcal{H}_{\|}^{\mathrm{eff}}$ exactly by the transfer-matrix method, we obtain the free energy per site,

$$f_{\mathrm{BEG}}(\eta,c,T)=-T\ln\lambda(\tilde{\Delta},\tilde{E},T)+J_{\perp}\eta^2+K_{\perp}c^2, \tag{4}$$

where $\lambda(\tilde{\Delta},\tilde{E},T)$ is the maximum eigenvalue of the transfer matrix for $\mathcal{H}_{\|}^{\mathrm{eff}}$, given by

$$\mathbf{T}=\begin{pmatrix} e^{\beta(J_{\|}+K_{\|}-\tilde{\Delta}-\tilde{E})} & e^{-\beta(\tilde{\Delta}+\tilde{E})/2} & e^{\beta(-J_{\|}+K_{\|}-\tilde{\Delta})} \\ e^{-\beta(\tilde{\Delta}+\tilde{E})/2} & 1 & e^{-\beta(\tilde{\Delta}-\tilde{E})/2} \\ e^{\beta(-J_{\|}+K_{\|}-\tilde{\Delta})} & e^{-\beta(\tilde{\Delta}-\tilde{E})/2} & e^{\beta(J_{\|}+K_{\|}-\tilde{\Delta}+\tilde{E})} \end{pmatrix}, \tag{5}$$

with $\beta=1/T$. Possible phase diagrams of the BEG model have been extensively studied through mean-field theories,[10,13] renormalization-group,[14] and transfer-matrix methods.[15] For the parameter regions relevant to the present case, $J_{\|}$, $J_{\perp}$, $K_{\|}$, $K_{\perp}$, and Δ are all positive, so that a solid-liquid-gas type phase diagram with proper slopes of transition lines is not obtained.

III. INTERCHAIN ELECTROSTRICTION

Then, we consider the interstack lattice degrees of freedom that have not explicitly been taken into account in Eq. (2). It is well known that an electrostriction effect potentially converts a continuous transition to a discontinuous one, since this gives rise to an additional negative free-energy term that contains the forth power of the relevant order parameter.[16] In the present case, we phenomenologically introduce an additional free energy,

$$f_{\mathrm{elst}}(c,y)=-\frac{e^2c^2}{b_0+y}+\frac{1}{2}M\Omega_{\perp}^2y^2, \tag{6}$$

where the first and second terms represent Coulomb attraction between the nearest-neighbor stacks[9] and the elastic energy for the distortion in the interstack direction. The reduced mass of TTF and CA molecule is M and $\Omega_{\perp}$ denotes the optical phonon frequency in the b-axis direction. Note that $f_{\mathrm{elst}}(c,0)$ has already been absorbed into $K_{\perp}$. The lattice constant without distortion is b_0, and y denotes the distortion. By minimizing $f_{\mathrm{elst}}(c,y)$ with respect to y, we obtain the optimized lattice constant,

$$b(T)=b_0+y(T)\sim b_0-\frac{\alpha}{2\beta}b_0c^2, \tag{7}$$

where we introduced energy scales of Coulomb and lattice processes, respectively, by

$$\alpha\equiv\frac{e^2}{b_0},\quad \beta\equiv\frac{1}{2}M\Omega_{\perp}^2b_0^2. \tag{8}$$

We thus have the energy gain due to the lattice distortion,

$$f_{\mathrm{elst}}(c,T)\sim-\varepsilon_{\mathrm{elst}}J_{\|}c^4, \tag{9}$$

where

$$\varepsilon_{\rm elst} \equiv \frac{\alpha^2}{4\beta J_\parallel}. \tag{10}$$

Using $M=1.85\times10^{12}$ Kg, $b_0=8.4\times10^{-10}$ m, and the fact that $\Omega_\perp$ may be larger than the optical phonon frequency in the *a*-axis direction $\Omega_\parallel=5.65\times10^{12}$ Hz,[6] we find a dimensionless electrostriction parameter is roughly given by $\varepsilon_{\rm elst}\sim0.01$.

Now, solving the self-consistent equations is reduced to searching (c,η) that gives the absolute minimum of the total free energy, $f(\eta,c,T)=f_{\rm BEG}(\eta,c,T)+f_{\rm elst}(c,T)$. The ionic phase is characterized by the ionicity condensation $c=1$, while the ferroelectric phase is characterized by $\eta\neq0$.

Note that, in the present scheme, any phase with $c\neq1$ is regarded as ''neutral'' and that the neutral phase has always $\eta=0$. In the BEG model, because of three states $p_{i,j}=0,\pm1$, c approaches the universal constant $c=2/3$ in the high-temperature limit, where the entropy term dominates the internal energy term. Therefore, in the parameter region where c continuously increases upon decreasing temperature, we have $2/3<c\leqslant1$. In the experiments,[1] the ionicity continuously increases upon decreasing temperature and jumps from $c\sim0.3$ to $c\sim0.6$ at the NIT. Thus, concerning the quantitative magnitude of the ionicity, there arises a difference between the experimental result and the present analysis. This apparent difference comes from the fact that we mapped the intrastack CT transfer and the DA dimerization onto the simple spin-1 Ising variables. Therefore, we should regard the difference as an artifact of the classical BEG model.

IV. NUMERICAL RESULTS AND PHASE DIAGRAM

From now on, we set $J_\parallel=1$ as an energy unit and the electric field E is set to be zero. In Fig. 1, we show the temperature dependence of c and η for various magnitudes of Δ with $K_\parallel=0.4$, $K_\perp=0.06$, $J_\perp=0.03$, and $\varepsilon_{\rm elst}=0.0095$. We introduce the condensation temperature $T_{\rm cond}$ and the crystallization temperature $T_{\rm cryst}$. The ionicity jumps into $c=1$ at $T_{\rm cond}$, while the ferroelectric order-parameter acquires a finite magnitude $\eta\neq0$ at $T_{\rm cryst}$. The ground state becomes ionic for $\Delta<1.49$. Both c and η exhibits a discontinuous change at the same transition temperature (the sublimation temperature) for $1.42<\Delta<1.49$. That is to say, $T_{\rm cond}=T_{\rm cryst}$. For $\Delta<1.42$, there appears a region, $T_{\rm cryst}<T<T_{\rm cond}$, where the system is ionic but still paraelectric. This region is identified with the $I_{\rm para}$ phase that is observed in TTF-CA under pressure. The point $(\Delta_t=1.42, T_t=0.45)$ is identified with the *triple point* (indicated by ''TP'' in Fig. 5). For $\Delta<1.42$, c still exhibits a discontinuous change at $T_{\rm cond}$, but η continuously evolves at $T_{\rm cryst}$, as shown in Fig. 1(c). The discontinuity jump of c becomes smaller and seems to vanish, as Δ decreases, as shown in Fig. 1(d). We stress that this discontinuity is a direct consequence of the weak but finite electrostriction effect. Without the electrostriction, as Δ decreases, $T_{\rm cond}$ and $T_{\rm cryst}$ continue to coincide with each other, and the transition simply changes from discontinuous to continuous at some critical value of Δ.[10,13–15]

As clearly seen from Eq. (7), about 0.5% discontinuous contraction of the interstack lattice constant (unit cell parameter b) is accompanied by the discontinuous jump of the ionicity. In Fig. 2, setting b_0 as a length unit, we show the temperature dependence of the unit cell parameter b given by Eq. (7), using the same parameter set as that in Fig. 1. Although the magnitude of the discontinuous contraction depends on the parameter choice of $\varepsilon_{\rm elst}$ and b_0, the qualitative nature (b jumps at $T_{\rm comd}$) does not change.

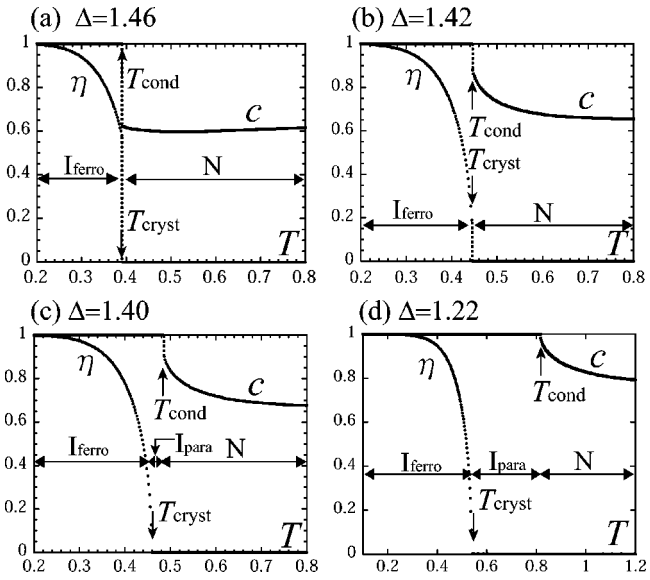

FIG. 1. Temperature dependence of c and η for various magnitudes of Δ with $K_\parallel=0.4$, $K_\perp=0.06$, $J_\perp=0.03$, and $\varepsilon_{\rm elst}=0.0095$. The condensation and crystallization temperature, $T_{\rm cond}$ and $T_{\rm cryst}$, respectively, are indicated. The vertical dotted lines indicate discontinuous jump of c and η. The temperature regions corresponding to $I_{\rm ferro}$), $I_{\rm para}$, and N phases are also indicated by horizontal arrows. Locations of the Δ values in (a)–(d) are indicated in the phase diagram of Fig. 5.

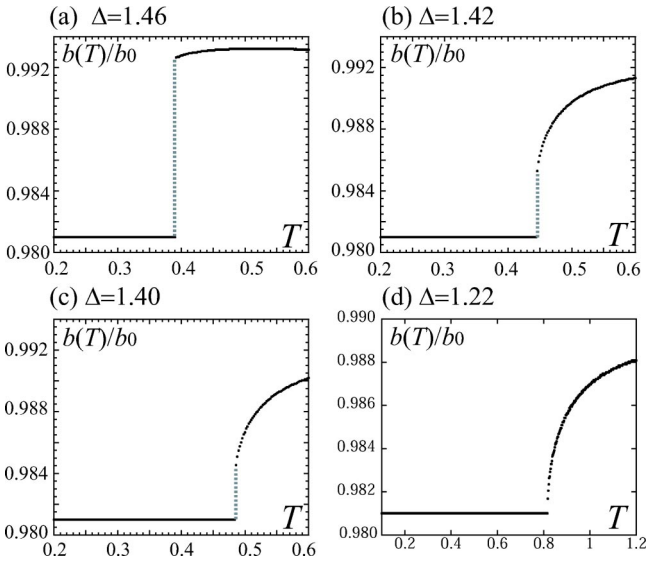

FIG. 2. Temperature dependence of the unit cell parameter b, $b(T)$. Locations of the Δ values in (a)–(d) are indicated in the phase diagram of Fig. 5.

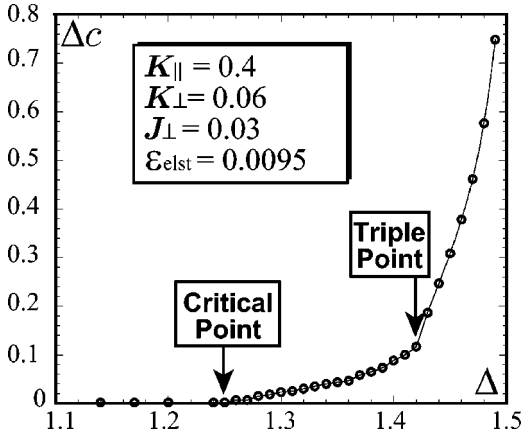

FIG. 3. Temperature dependence of the discontinuity of the ionicity, Δc.

To see the discontinuity of the ionicity more closely, we show in Fig. 3 the Δ dependence of the discontinuity at the condensation temperature, Δc. It is clearly seen that Δc decreases as Δ decreases and eventually reaches zero at $\Delta = 1.25$. For $\Delta < 1.25$, the condensation occurs without ionicity jump. Then, the lattice contraction at $T_{\rm cond}$ also becomes continuous. Therefore, $\Delta = 1.25$ with the corresponding $T_{\rm cond} = 0.76$ is identified with a *critical point* (indicated by "CP" in Fig. 5). This critical point is in fact a critical end point discussed by Fisher and Barbosa.[17] This result is well consistent with the experimental fact that the ionicity jump finishes at the critical point.[2]

The dielectric constant is given by $\varepsilon = 1 + 4\pi\alpha$, where the uniform polarizability is $\alpha = 1/T\Sigma_{i,j}\Sigma_{l,m}[\langle p_{i,j}p_{l,m}\rangle - \langle p_{i,j}\rangle\langle p_{l,m}\rangle] = (c - \eta^2)/T$. In Fig. 4, we show the temperature dependence of α for various magnitudes of Δ. It is seen that along the N-$I_{\rm ferro}$ boundary, the polarizability exhibits a sharp single cusp at $T_{\rm cond} = T_{\rm cryst}$. For $\Delta_c < \Delta < \Delta_t$, a discontinuous jump occcurs at $T = T_{\rm cond}$ and a cusp at $T = T_{\rm cryst}$. The discontinuity at $T = T_{\rm cond}$ finishes at $\Delta = \Delta_c$. Here, we should mention that the BEG model of dipoles misses all *delocalization effects*. This may cause the apparently small polarizability peaks of order unity as seen in Fig. 4 at transitions.

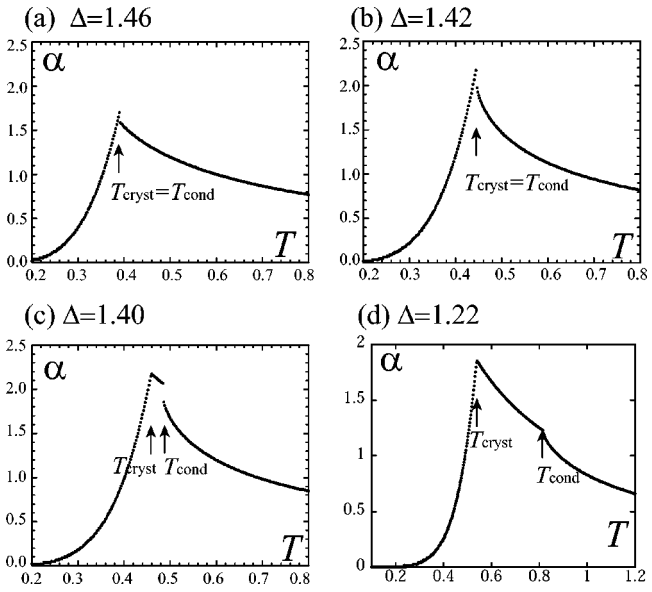

FIG. 4. Temperature dependence of the polarizability, α. Locations of the Δ values in (a)–(d) are indicated in the phase diagram of Fig. 5.

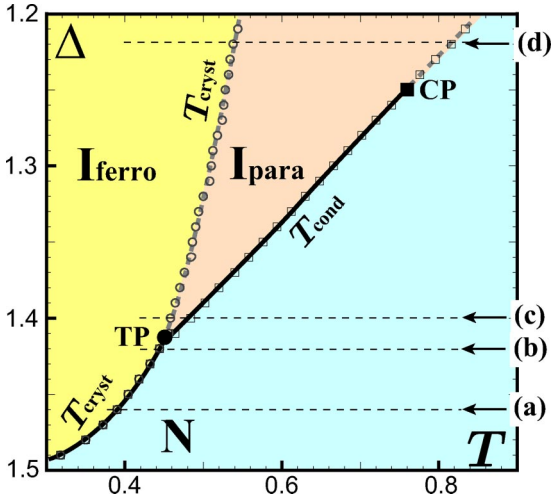

FIG. 5. (Color online) Phase diagram for $K_{\|} = 0.4$, $K_{\perp} = 0.06$, $J_{\perp} = 0.03$, and $\varepsilon_{\rm elst} = 0.0095$. The solid and dashed lines represent discontinuous and continuous transitions, respectively. TP and CP represent the triple point and the critical point, respectively. Locations of the Δ values used in (a)–(d) of Figs. 1, 2, and 4 are indicated by the horizontal arrows.

In Fig. 5, we show the phase diagram of the system for $K_{\|} = 0.4$, $K_{\perp} = 0.06$, $J_{\perp} = 0.03$, and $\varepsilon_{\rm elst} = 0.0095$. Regarding the decreasing Δ as increasing pressure, this phase diagram is consistent with the experimentally found, pressure-temperature phase diagram of TTF-CA.[2] The triple point, the critical point, and the observed interstack lattice contraction are reproduced. For simplicity, we here ignored the change of Δ due to thermal lattice contraction. Exactly speaking, to convert our Δ-T phase diagram to a P-T diagram, we need to take account of the temperature dependence of Δ, $\Delta(T)$. By appropriately treating $\Delta(T)$, we may obtain the corresponding P-T phase diagram satisfying the Clausius-Clapeyron relation. We stress that, even when we take this simple view, a qualitative nature of the phase diagram is not changed. Identifying the triple point $(\Delta_t, T_t) = (1.42, 0.45)$ with the experimentally obtained one $(P_t, T_t) \sim (500\ \text{MPa}, 210\ \text{K})$, we see that our parameter choice here corresponds to $K_{\perp} = 28$ K and $J_{\perp} = 14$ K.

Lajzerowicz and Sivardiére[18] extensively developed a mean-field analysis of the BEG model and obtained liquid-gas-solid like phase diagrams on the P-T plane. However, they considered a lattice gas analog of a simple fluid, where the physical pressure of the lattice gas is simply given by $-f$, with f being the Helmholtz free energy per volume. In the present context, the pressure of the spin system has no physical meaning and the phase diagram obtained by Lajzerowicz and Sivardiére cannot be applied to TTF-CA.

V. CONCLUDING REMARKS

In the present work, to simulate a pressure-temperature phase diagram of the quasi-one-dimensional mixed-stack charge-transfer (CT) complex TTF-CA,[2,3] we have studied the quasi-one-dimensional spin-1 Blume-Emery-Griffiths (BEG) model. In this scheme, the electric dipoles on a DA pair is described by classical dipoles, which is apparently far from the microscopic Peierls-Hubbard model[7,19] that have been applied to the ground-state properties of TTF-CA. This simplification means that all *delocalization effects* are missing in the present scheme. This may cause the apparently small polarizability peaks of order unity as seen in Fig. 4 at transitions. To overcome these flaws, we need to go back to the microscopic Peierls-Hubbard model[7,19] and make clear the interplay of low-energy spin and charge-transfer dynamics.

We should also mention that all the microscopic degrees of freedom of spin and charge are not explicitly treated in our scheme and consequently any magnetic degrees of freedom are frozen out. Accordingly, the spin and charged solitons or neutral-ionic domain walls, which are elementary excitations in one-dimension,[7] are not incorporated in the present scheme. It is naturally expected that in quasi-one-dimensional case, such one-dimensional excitations dissociate and eventually lead to ferroelectric phase. To elucidate this dimensionality-driven process may be required to fully describe the ferroelectric phase transition in TTF-CA. This is quite an involved problem. We keep this for future project.

Although we have the above apparent drawbacks, we may say that our simple model rationalizes an essential point of the multicritical behavior of TTF-CA, i.e., the interchain electrostriction (Coulomb-lattice coupling) *exclusively* enhances the charge concentration (ionicity condensation), but does not affect the interchain ferroelectric coupling. This is the main reason why the intermediate paraelectric ionic (I_{para}) phase appeared in between the neutral (N) and ferroelectric ionic (I_{ferro}) phases on the Δ-T phase diagram. This scenario addressed here may give a canonical example of a ''critical phase control in many-electron system,'' where the phase transition and criticality are controlled by changing such a microscopic parameter as an electrostriction.

This work was partly supported by a Grant-in-Aid for Scientific Research (C) from Japan Society for the Promotion of Science. T.L. wishes to acknowledge hospitality at the Institute for Molecular Sciences, Okazaki, and thank colleaugues for creating a pleasant and stimulating environment there.

[1] J.B. Torrance, J.E. Vazquez, J.J. Mayerle, and V.Y. Lee, Phys. Rev. Lett. **46**, 253 (1981).
[2] M.H. Lemée-Cailleau, M. Le Cointe, H. Cailleau, T. Luty, F. Moussa, J. Roos, D. Brinkmann, B. Toudic, C. Ayache, and N. Karl, Phys. Rev. Lett. **79**, 1690 (1997).
[3] T. Luty, H. Cailleau, S. Koshihara, E. Collet, M. Takesada, M-H. Lemée-Cailleau, M. Buron-Le Cointe, N. Nagaosa, Y. Tokura, E. Zienkiewicz, and B. Ouladdiaf, Europhys. Lett. **59**, 619 (2002).
[4] S. Koshihara, Y. Tokura, K. Takeda, and T. Koda, Phys. Rev. Lett. **68**, 1148 (1992).
[5] E. Collet, M.H. Lemee-Cailleau, M. Buron-Le Cointe, H. Cailleau, M. Wulff, T. Luty, S. Koshihara, M. Meyer, L. Toupet, P. Rabiller, and S. Techert, Science **300**, 612 (2003).
[6] T. Iizuka-Sakano and Y. Toyozawa, J. Phys. Soc. Jpn. **65**, 671 (1996).
[7] N. Nagaosa, J. Phys. Soc. Jpn. **55**, 3488 (1986).
[8] T. Luty in *Relaxations of Excited States and Photo-Induced Structural Phase Transitions*, edited by K. Nasu, Springer Series in Solid-State Sciences Vol. 124 (Springer-Verlag, 1996), p. 142.
[9] T. Kawamoto, T. Iizuka-Sakano, Y. Shimoi, and S. Abe, Phys. Rev. B **64**, 205107 (2001).
[10] M. Blume, V.J. Emery, and R.B. Griffiths, Phys. Rev. A **4**, 1071 (1971).
[11] H.M. McConnel, B.M. Hoffman, and R.M. Metzger, Proc. Natl. Acad. Sci. U.S.A. **53**, 46 (1965).
[12] D.J. Scalapino, Y. Imry, and P. Pincus, Phys. Rev. B **11**, 2042 (1975).
[13] W. Hoston and A.N. Berker, Phys. Rev. Lett. **67**, 1027 (1991).
[14] A.N. Berker and M. Wortis, Phys. Rev. B **14**, 4946 (1976)
[15] E. Albayrak and M. Keskin, J. Magn. Magn. Mater. **213**, 201 (2000).
[16] See, for example, P. W. Anderson, *Basic Notions of Condensed Matter Physics* (Addison-Wesley, Reading, MA, 1984), Sec. 2 C.
[17] M.E. Fisher and M.C. Barbosa, Phys. Rev. B **43**, 11 177 (1991); M.C. Barbosa and M.E. Fisher, *ibid.* **43**, 10 635 (1991).
[18] J. Lajzerowicz and J. Sivardière, Phys. Rev. A **11**, 2079 (1975).
[19] N. Miyashita, M. Kuwabara, and K. Yonemitsu, cond-mat/0211487, J. Phys. Soc. Jpn. (to be published).